Electronic Supporting Information

Hybrid alginate-industrial waste spheres for the adsorption and reuse of methylene blue

Paulo H. S. Lopes[1]*, Joyce M. G. da Costa[2], Alexandre S. V. da Costa[3]

[1]*Universidade Federal dos Vales do Jequitinhonha e Mucuri, Postgraduate Program in Biofuels, Diamantina, Minas Gerais, Brazil. ORCID: 0000-0003-1461-0208*

[2]*Universidade Federal dos Vales do Jequitinhonha e Mucuri, Institute of Science and Technology, Diamantina, Minas Gerais, Brazil. ORCID: 0000-0002-8936-6142*

[3]*Universidade Federal dos Vales do Jequitinhonha e Mucuri, Postgraduate Program in Biofuels, Teófilo Otoni, Minas Gerais, Brazil. ORCID: 0000-0001-7251-7816*

*Corresponding author: Rodovia MGT 367 - Km 583, nº 5.000 Alto da Jacuba, Diamantina, Minas Gerais, Brazil – 39100000. Phone: +5538997436426. E-mail adresses: paulo.lopes@ufvjm.edu.br. Orcid: https://orcid.org/0000-0003-1461-0208

Table of Contents

1 Waste materials employed in the initial screening

Waste samples were obtained through partnerships with various companies in the state of Minas Gerais, Brazil, selected based on local availability via simple random sampling and identified according to local nomenclature.

The following materials were grouped as lignocellulosic waste: 1 - In natura eucalyptus sawdust (powder from sawmills); 2 - Cenibra charcoal mulch (charcoal residue from Celulose Nipo-Brasileira S.A.); 3 - Primary sludge fibers (lignocellulosic fiber residues from Celulose Nipo-Brasileira S.A.).

The mineral wastes evaluated were: 1 - Grão Mogol phyllite (metamorphic rock powder extracted from a white granite area in Minas Gerais); 2 - Positive sludge +Fe (iron-enriched sludge extracted via wet processing and iron extraction in a mining plant); 3 - Toledo filter press (sludge dehydrated by a press system from Toledo Mineração); 4 - MIII CBL (residue containing a mixture of mica, muscovite, and feldspar generated by mineral processing at Companhia Brasileira de Lítio); 5 - Silicate (silicated fraction discarded during lithium extraction by Companhia Brasileira de Lítio); 6 - Pulverized sand +Fe (iron-enriched sand extracted via wet processing and iron extraction in a mining plant); 7 - CBL baghouse filter dust (fine powder collected from industrial exhaust systems at Companhia Brasileira de Lítio); 8 - MIII Muscovite (muscovite fraction extracted by sieving the tailings from initial spodumene processing); 9 - Positive sand -Fe (pulverized sand with low iron content due to magnetic separation); 10 - Mixed ornamental rock cutting powder (waste generated by stonemasons containing granite, marble, and quartzite).

All raw materials were subjected to oven-drying (50 °C for 24 h for moisture removal). Inorganic raw materials were ground in a Brastorno MAXMILL disc pulverizer mill (Brazil). Lignocellulosic raw materials were ground in a Tecnal R-TE-650/1 Wiley-type macro mill (Brazil). Materials were sieved using ISO 3310/1 sieves (≤90 μm, 170 mesh) for particle size classification. All reagents employed were of analytical grade (A.R.).

2 Formulation and optimization of hybrid matrices

For bead production, screening experiments were initially conducted to optimize composition and preparation conditions.

2.1 Screening of inorganic residual additives in hybrid matrix composition

This experiment aimed to evaluate the effect of different additives on the adsorption matrix. The base matrix consisted of sodium alginate, with the second component (inorganic residue) being varied.

Matrices were formulated by dispersing 1.0 g of sodium alginate and 0.5 g of residue in 100 mL of distilled water. Initially, the residue was dispersed in 20 mL of distilled water at room temperature; then, the alginate was added, forming a homogeneous, lump-free paste. Subsequently, the remaining water was added to produce a homogeneous solution. The mixture was kept stationary at room temperature for 1 h to ensure complete homogenization and the release of air bubbles.

Next, the mixture was dripped using a 10 mL burette into 50 mL of a 1% (w/v) calcium chloride solution to promote cross-linking. The formed beads remained in the cross-linking solution for 30 min. After this period, the material was washed with distilled water and stored under refrigeration for subsequent tests. The matrices were evaluated via methylene blue (MB) adsorption tests.

2.3 Screening of lignocellulosic waste in hybrid matrix composition

This experiment aimed to evaluate the effect of different lignocellulosic residues on the adsorption matrix. The base matrix consisted of sodium alginate and the inorganic additive (as determined in the screening in Section 2.2), while the third component (lignocellulosic residue) was varied.

The matrices were formulated by dispersing 1.0 g of sodium alginate, 0.5 g of the inorganic additive, and 0.5 g of lignocellulosic residue in 100 mL of distilled water. Initially, the residue and the additive were dispersed in 20 mL of distilled water at room temperature; then, the alginate was added to form a homogeneous, lump-free paste. The remaining water was added gradually to produce a homogeneous solution. The mixture was held at room temperature for 1 h to achieve complete homogenization and remove air bubbles.

Subsequently, the polymer solution was dripped via a 10 mL burette into 50 mL of a 1% (w/v) calcium chloride solution for cross-linking. The beads were incubated in the solution for 30 min, washed with distilled water, and refrigerated. The matrices were evaluated via methylene blue adsorption tests.

2.4 Preparation method for the ternary adsorption matrix

Initially, the residual aluminum silicate (AS) powder was added to the preparation vessel before water, and the mixture was dry-blended with the primary sludge fibers (PF) (Steps 1-2). Next, a portion of the distilled water was added to allow for the initial hydration of both components (Step 3). Alginate was then incorporated and stirred until a homogeneous paste was obtained (Steps 4-5). Finally, the water volume was topped up to reach the target concentration for each formulation (Steps 6-7) (Fig. S1). This simple mixing method (without the use of sophisticated equipment) was developed to ensure better adjustment of the mixture and prevent component separation or gradients, as established in preliminary tests.

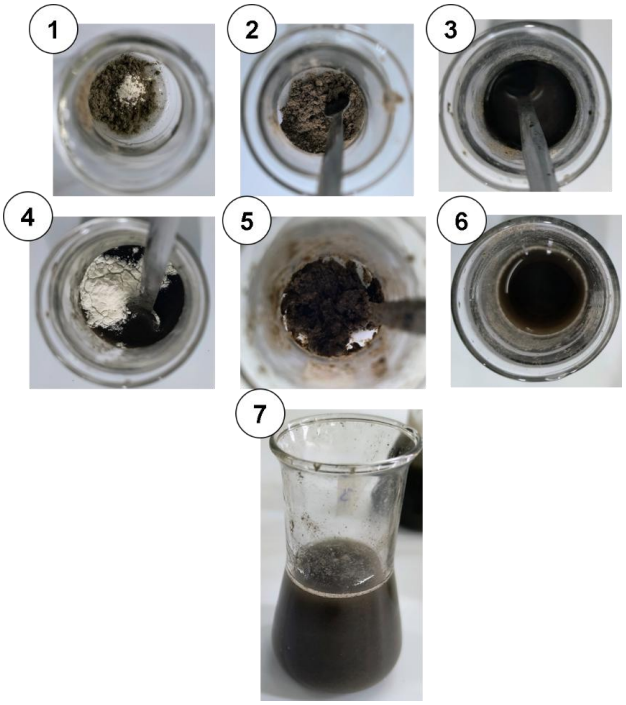

Fig. S1. Preparation sequence of the solution containing the constituents for adsorbent bead formation. Conditions: (1-2) mixing order = Silicate+Fibers → (3) Water → (4) Alginate → (5-7) final concentrations as per Table 1.

2.5 Equations employed in adsorption analysis

Following MB adsorption, the objective was to determine the amount of dye available before and after dilution. Accordingly, the formulas expressed below were employed, respecting the determination order of each variable. Absorbance (ABS) was used to measure the MB concentration in the diluted solution (considering dilutions to maintain ABS within the stipulated detection range of 0-1). The steps were as follows: (1) convert ABS to $C_{diluted}$ (mg L^{-1} in the diluted solution); (2) multiply by the dilution volume ($V_{dilution}$) to obtain the mass in the diluted solution; (3) this mass corresponds to the amount present in the MB solution without dilution; (4) the concentration of the original solution was determined by dividing this mass by the aliquot volume ($V_{aliquot}$); (5) subsequently, the adsorption capacity Q (mg g^{-1}) was calculated (Table S1).

Table S1. Calculation steps for determining MB adsorption capacity

Determination of the diluted concentration in the aqueous volume for each individual assay	$C_{diluted,i} = ABS_i/0{,}1417$
Determination of the original concentration in the initial MB aliquot	$C_{original,i} = C_{diluted,i} * Dilution$
	$Dilution = \frac{V_{dilution}}{V_{aliquot}}$
Determination of the adsorption capacity (mg g^{-1}) for each individual assay	$Qi\left(\frac{mg}{g}\right) = \frac{\left(C_{original,0} - C_{original,essay\ i}\right) * \left(\frac{V_{aliquot}}{1000}\right)}{m_{dry,i}}$
	Where, *i* refers to individual samples; *MB* refers to methylene blue; *eq* (from equilibrium) refers to isotherm data; *t* (from time) refers to kinetic data. $C_{original,0}$ is equivalent to the values obtained for the blank assays (without adsorbent), representing the concentration prior to the adsorption process; $C_{original,essay\ i}$ is equivalent to the values obtained for each individual assay
	(*i* = Controls, 1, 2, 3..., *n*);
	$V_{aliquot}$/1000 refers to the volume of MB in contact with the beads for 4 h, measured in L;
	$m_{dry,i}$ is the mass of the adsorbent in assay after drying at 40 °C for 24 h.
Determination of the MB removal efficiency	$\%R = \frac{\left(C_{original,0} - C_{original,essay\ i}\right)}{C_{original,0}} * 100$
Non-linear mathematical models of adsorption isotherms	Langmuir Isotherm: $Q_{eq} = \frac{Q_{max}K_L C_{eq}}{1+K_L C_{eq}}$
	Freundlich Isotherm: $Q_{eq} = K_F C^{\frac{1}{n}}{}_{eq}$
	Temkin Model: $Q_{eq} = Bln(K_T C_{eq})$
	Sips Model: $Q_{eq} = \frac{Q_{max}\left(K_S C^{n_S}{}_{eq}\right)}{1+K_S C^{n_S}{}_{eq}}$
Non-linear mathematical models for kinetic data fitting	Pseudo-first-order: $Q_t = Q_{eq}(1 - e^{-k_1 t})$
	Pseudo-second-order: $Q_t = \frac{Q_{eq}^2 k_2 t}{1+Q_{eq}k_2 t}$
	Elovich: $Q_t = \frac{1}{\beta}\ln(1 + \alpha\beta T)$
	Intraparticle diffusion: $Q_t = k_{id}t^{\frac{1}{2}} + C$
	Kinetic Avrami: $Q_t = Q_{eq}(1 - e^{-(k_{av}t)^{n_{av}}})$

Source: Adapted from Holliday et al. 2024; Mikolajczyk et al. 2024; Ostaszewski et al. 2022; Vitek and Masini 2023.

2.6 Adsorption efficiency (dry *vs.* wet beads)

The removal efficiency of the MB dye by wet and dry beads was determined using the same mass of adsorbent, calculated on a dry basis. Drying the wet beads normalizes adsorption results relative to the dry mass, avoiding biases associated with the inherent moisture variation of newly formed beads.

Dry (D) beads were obtained through a procedure designed to preserve structural integrity and porosity. Wet (W) beads intended for drying underwent a gradual solvent exchange via sequential immersion in ethanol solutions at 30%, 50%, 70%, and 100% (v/v), remaining for 45 minutes in each concentration to reduce surface tension and prevent the collapse of the porous structure (Li et al. 2021; Wei et al. 2025). Subsequently, the samples were dried at room temperature (~20 °C) until a constant mass was reached. Each adsorption assay received a mass equivalent to 50 mg of dry material, previously calculated for the wet beads based on moisture content. The MB adsorption process followed the same procedure described previously, maintaining negative and positive controls.

3.1 Formulation and optimization of hybrid matrices

The formulated beads were evaluated for their methylene blue adsorption capacity, as it is a dye characterized by ease of handling, analytical reliability, and environmental representativeness, and is widely used to describe the adsorption mechanisms of adsorbent materials. Therefore, it serves as an indicator for the initial screening of the adsorption performance of novel materials.

3.1.1 Screening of inorganic residual additives

Fig. S2 shows the results regarding the methylene blue (MB) adsorption capacity analysis for the different formulations. The evaluation of MB adsorption capacity by the various inorganic supports incorporated into the polymeric matrix revealed statistically significant differences between assays, confirmed by analysis of variance (ANOVA). The results show that the highest performance was obtained with silicate (R5), at 15.85 mg g^{-1}, which was statistically equivalent to iron-enriched pulverized sand (R6) and the MIII CBL material (R4). The positive control (C+), consisting of pure alginate beads, exhibited intermediate performance (14.70 mg g^{-1}), surpassing some residues but remaining inferior to the aforementioned materials.

The presence of distinct groups suggests that the mineralogical nature of the residues plays a crucial role in the cationic dye's affinity for them. In the case of silicate (R5), the high performance may be associated with the presence of silanol groups (Si–OH), which favor electrostatic interactions and hydrogen bonding with methylene blue, as well as a possible contribution from porosity. The pulverized sand +Fe (R6), in turn, likely presents an increase in surface negative charges due to the presence of oxides/hydroxides, which intensify electrostatic attraction with the cationic dye.

The fact that the positive control (C+) exhibited a capacity close to residues such as CBL baghouse filter dust (R7) and mixed ornamental rock cutting powder (R10) highlights that alginate itself possesses active sites, primarily carboxylic groups, capable of interacting with methylene blue.

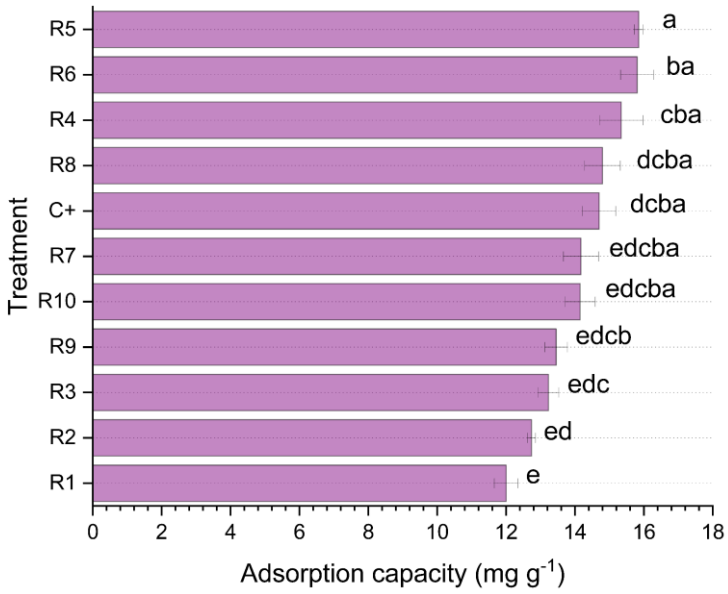

Fig. S2. Adsorption capacity (*Q*) measured in mg of methylene blue per g of dry support, varying the inorganic residues. The treatment numbers (R_i = C+, 1, 2, …) in the figure refer to: 1 – Grão Mogol phyllite; 2 – Positive sludge +Fe; 3 – Toledo filter press; 4 – MIII CBL; 5 – Silicate; 6 – Pulverized sand +Fe; 7 – CBL baghouse filter dust; 8 – MIII Muscovite; 9 – Positive sand -Fe; 10 – Mixed ornamental rock cutting powder. (C+) is the positive control, containing pure alginate beads; the negative control or C_0 was the absence of adsorbent material, with a concentration equal to 332 ± 12 mg L^{-1}. Analysis of variance (ANOVA) revealed significant differences between assays (*p*-value < 0.05), as the $F_{calculated}$ exceeded the $F_{tabulated}$ value (6.72, with $F_{tabulated}$ for 10/33 degrees of freedom equal to 2.14), and a coefficient of variation of 6.80% (maintained below 10%). Superscripts “a” through “f” indicate statistically distinct or similar groups. Conditions: (MB) = 332.00 mg L^{-1}; dosage = 1.00 g alginate + 0.50 g residue per 100 mL; pH = 6.98 ± 0.08; temperature = 292 K; contact time = 4 h.

3.1.2 Screening of lignocellulosic waste as adsorption matrix components

Fig. S3 presents a comparative analysis of adsorption capacity across different treatments, highlighting statistically significant differences indicated by the grouping letters from the multiple-comparison test. Treatments R3 and R6 exhibited the lowest adsorption means and did not differ statistically; this suggests that, despite structural or compositional differences between the two assays, their performance was equivalent and limited. Subsequently, treatments C+1 (14.18 mg g^{-1}) and R7 (14.28 mg g^{-1}) showed the highest observed values and were not statistically different from each other (Group a). Tukey’s test indices suggest that PF, with R7 showing lower experimental error, enhances the composite's adsorptive capacity, whereas residues with less chemical modification (R3 and R6) exhibit limited performance.

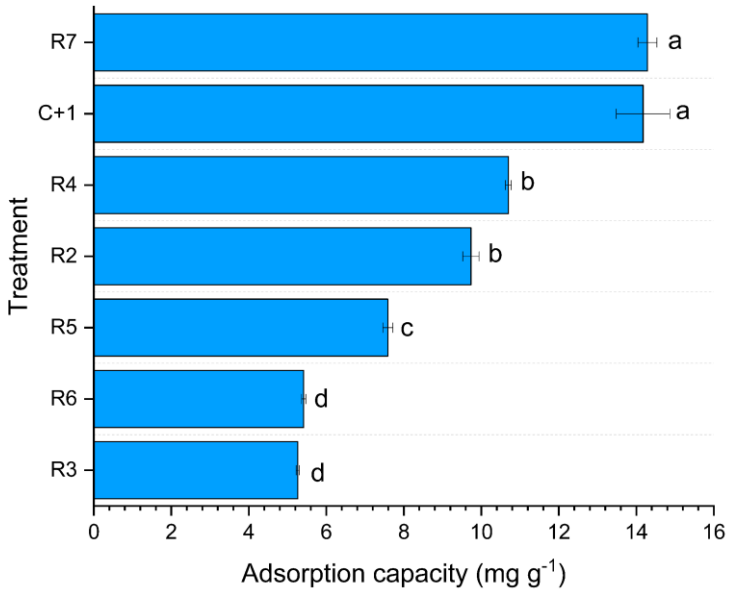

Fig. S3. Adsorption capacity (Q) measured in mg of methylene blue per g of dry support, varying the lignocellulosic residues. The labeled assays consist of the alginate + silicate + [residue] composition: C+1 is the positive control (formulation obtained in experiment 1); R2 is *in natura* sawdust with a particle size < 115 µm; R3 is sawdust treated with 3% (w/v) sodium hydroxide; R4 is sawdust treated with sodium hydroxide and functionalized with citric acid (particle size of 250 µm); R5 is sawdust treated with sodium hydroxide and functionalized with citric acid (particle size < 115 µm); R6 is Cenibra charcoal mulch; and R7 is primary sludge fiber residue. The negative control (C_0) consisted of the dye solution without adsorbent material, with a concentration of 332 ± 12 mg L^{-1}. Analysis of variance (ANOVA) revealed significant differences between assays (p-value < 0.05), with a coefficient of variation = 6.51%, which is < 10%. The $F_{calculated}$ (108.36) was higher than the $F_{tabulated}$ (2.85 for 6/14 degrees of freedom). Superscripts “a” through “d” indicate statistically distinct groups. Conditions: (MB) = 332.00 mg L^{-1}; dosage = 1.00 g alginate + 0.50 g silicate + 0.50 g fiber per 100 mL; pH = 6.98 ± 0.08; temperature = 292 K; contact time = 4 h.

These results suggest that the conditions applied in these treatments, possibly related to higher active site availability, more favorable surface characteristics, or enhanced chemical interaction with the adsorbate, were decisive for the superior performance.

In general, the observed pattern highlights a gradient in adsorptive capacity among the treatments, reinforcing the influence of the matrices' structural and/or chemical parameters. Furthermore, the proximity between the means of C+1 and R7 suggests a potential saturation effect, in which further increases in the controlled variables do not yield significant capacity gains, possibly due to intrinsic limitations of active sites or dye diffusion within the matrix.

3.1.3 Experimental design: Rotatable Central Composite Design (RCCD)

Table S2. Numerical results for viscosity (cP) and adsorption capacity (Q) for the 17 RCCD trials and the positive control

Run	Primary sludge fibers (%, w/v)	Aluminum silicate (%, w/v)	Viscosity (cP)	Q (mg g^{-1})
1	0.4000	0.2000	1,671	16.3710
2	0.4000	0.5000	10,174	14.7992
3	1.5000	0.2000	2,363	10.9760
4	1.5000	0.5000	73,664	6.9292
5 (C)	0.9500	0.3500	10,618	12.8152
6	0.4000	0.2000	1,428	18.8492
7	0.4000	0.5000	10,474	13.6668
8	1.5000	0.2000	4,211	11.9965
9	1.5000	0.5000	64,426	9.4240
10 (C)	0.9500	0.3500	9,430	12.2769
11	0.0297	0.3500	5,003	19.0554
12	1.8703	0.3500	44,151	8.8917
13	0.9500	0.0990	731.8000	15.3359
14	0.9500	0.6010	70,905	5.7473
15	0.9500	0.3500	9,298	13.4905
16	0.9500	0.3500	9,310	11.1825
17 (C)	0.9500	0.3500	9,011	13.0447
Control +	0.5000	0.5000	11,446	14.4140

Table S3. Effects table, regression coefficients, and significant factors for the RCCD

Factors	Effect	Pure Error (Effect)	Regression Coefficients	Pure Error (Coeff.)	$t_{calculated}$	p-value
Mean	12.666	0.227	12.666	0.227	55.813	0.000
x_1	-6.084	0.214	-3.042	0.107	-28.463	0.001
x_1^2	1.184	0.236	0.592	0.118	5.012	0.038
x_2	-4.326	0.214	-2.163	0.107	-20.241	0.002
x_2^2	-1.267	0.236	-0.634	0.118	-5.363	0.033
x_3	0.180	0.214	0.090	0.107	0.841	0.489
x_3^2	0.015	0.236	0.007	0.118	0.063	0.956
$x_1.x_2$	0.034	0.279	0.017	0.139	0.121	0.915

$x_1.x_3$	-0.534	0.279	-0.267	0.139	-1.917	0.195
$x_2.x_3$	0.542	0.279	0.271	0.139	1.946	0.191

Where: x_1 represents primary sludge fibers, x_2 represents residual aluminum silicate, and x_3 represents calcium chloride dihydrate.

Table S4. ANOVA table for the RCCD results

Source of Variation	**Sum of Squares**	**Degrees of Freedom**	**Mean Square**	F_{calc}	F_{tab}	F_{calc}/F_{tab}	***p*-value**
Regression	202.412	6.000	33.735	22.376	3.220	6.949	0.000
Residuals	15.076	10.000	1.508				
Lack of Fit	14.766	8.000	1.846	11.883	19.370		
Pure Error	0.311	2.000	0.155				
Total	217.488	16.000					
R^2	0.931						

The interpretation of this table is as follows: 1- The R^2 exceeds the established limit (75%); 2- The *p*-value is lower than the significance level (0.05); 3- The F_{calc}/F_{tab} ratio indicates predictive capacity, as the ratio is greater than 3, allowing for the presentation of all results related to the contour plots. These findings are supported by the Fisher-Snedecor F-test, where the regression F_{calc} is higher than the associated F_{tab}, and the lack-of-fit F_{calc} is lower than the associated F_{tab}.

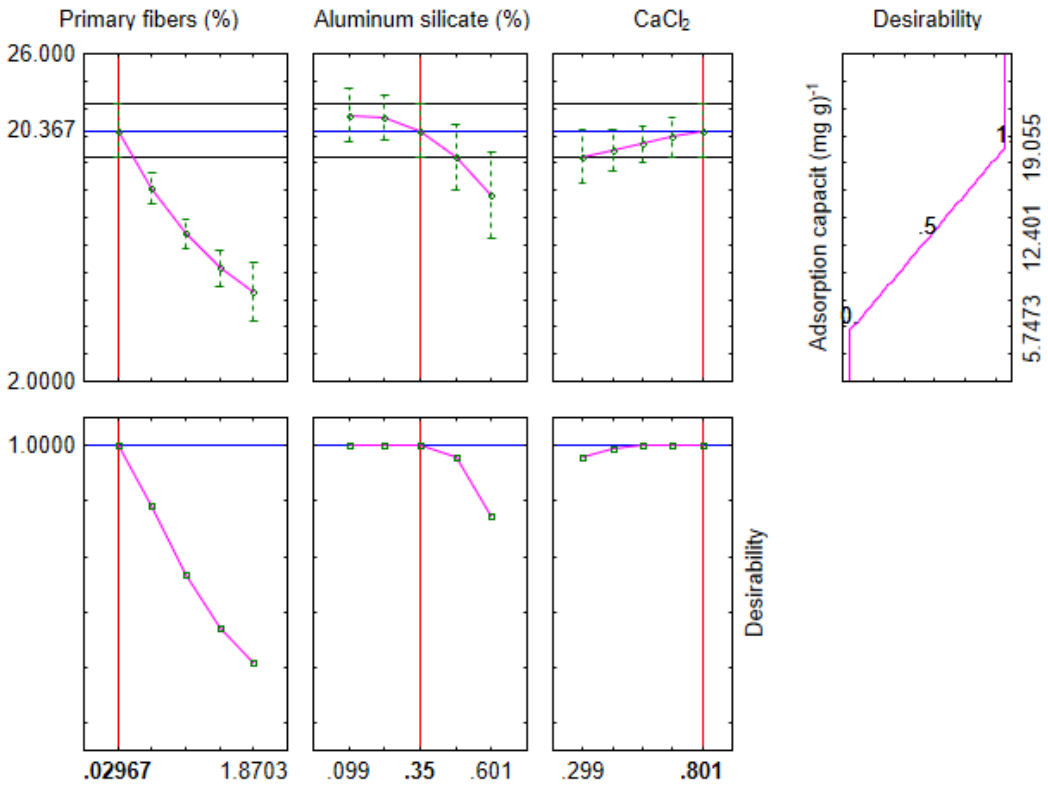

Fig. S4. Desirability and optimization by RCCD: determination of bead composition to maximize adsorption capacity (*Q*) in mg of methylene blue per g of dry support. “Primary sludge fibers” is “Primary fibers”. Concentrations expressed as percentages refer to weight by volume (w/v). Conditions: (MB) = 332.00 mg L^{-1}; dosage = 18 beads mL^{-1}; temperature = 292 K; time = 4 h.

3.1.4 Methylene blue removal efficiency of the validated formulation beads

According to Table S5, the general trend indicates that wet beads promote higher MB removal than dry beads. The results suggest that the hydrated state of the beads, combined with an appropriate fiber blend and low-to-moderate Ca^{2+} cross-linking, is a key factor in maximizing MB removal. Formulations F2-W, F3-W, and F4-W constitute a statistically significant block (Group “a”), demonstrating that it is possible to outperform pure calcium alginate if the microstructure is correctly engineered.

This systematic difference indicates that the hydration state significantly alters the availability of adsorption sites and the diffusion of MB. Wet beads maintain a swollen polymeric network with larger pores and more favorable diffusion paths, whereas the drying process tends to cause shrinkage, pore collapse, physical entrapment, and a reduction in accessible surface area.

Table S5. Methylene blue (MB) removal efficiency for beads based on formulations 1 to 4

Assay/Formulation	Bead (D/W)	MB Removal Efficiency (%)
F1	D	48.781 ± 3.881^{d}
F2	D	65.418 ± 2.246^{cb}
F4	D	72.044 ± 3.324^{cb}
C+	D	75.811 ± 0.433^{b}
F3	D	76.656 ± 2.875^{b}
C+	W	71.120 ± 1.756^{cb}
F1	W	73.420 ± 0.906^{b}
F2	W	85.551 ± 0.131^{a}
F3	W	87.304 ± 0.337^{a}
F4	W	92.670 ± 0.976^{a}

Legend: The positive control (C+) consisted of calcium alginate to verify the extent to which the formulations improve MB removal from aqueous solution. ANOVA revealed significant differences between assays (*p*-value < 0.05, coefficient of variation = 3.45%). F_{calc} (68,95) was higher than F_{Tab} (2.39 for 9/20 degrees of freedom). Superscripts “a” through “d” indicate statistically distinct groups. Each assay follows the described composition: F1 (0.03 % PF; 0.35 % AS; 0.80 % $CaCl_2$; 1% alginate); F2 (0.40% PF; 0.20% AS; 0.70% $CaCl_2$; 1% alginate); F3 (0.40% PF; 0.20% AS; 0.40% $CaCl_2$; 1% alginate); F4 (1.50% PF; 0.20% AS; 0.40% $CaCl_2$; 1% alginate). Concentrations expressed as percentages refer to weight by volume (w/v).

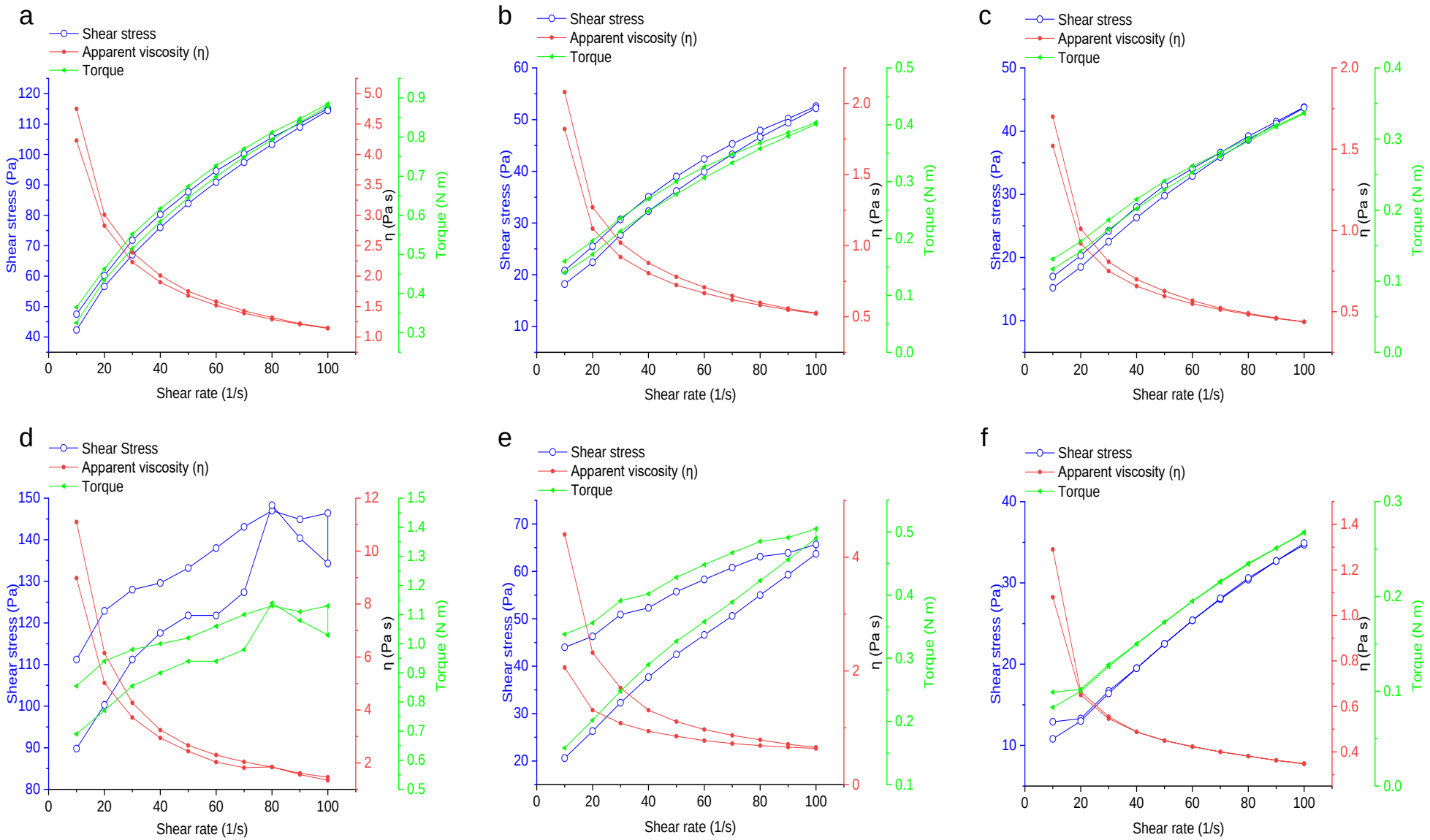

Fig. S5. Plots of shear stress, apparent viscosity, and torque versus shear rate for each formulation: (a) F1, (b) F2, (c) F3, (d) F4, (e) F5, (f) F6. F1 (0.03 % PF; 0.35 % AS; 0.80 % $CaCl_2$; 1% alginate); F2 (0.40% PF; 0.20% AS; 0.70% $CaCl_2$; 1% alginate); F3 (0.40% PF; 0.20% AS; 0.40% $CaCl_2$; 1% alginate); F4 (1.50% PF; 0.20% AS; 0.40% $CaCl_2$; 1% alginate); F5 (0.50% AS; 1.00% $CaCl_2$; 1% alginate); e F6 (1.50% PF; 1.00% $CaCl_2$; 1% alginate). Concentrations in (w/v). Conditions: temperature = 20.0 °C; stabilization = 2 min; shear rate sweep = 10 to 100 s^{-1}.

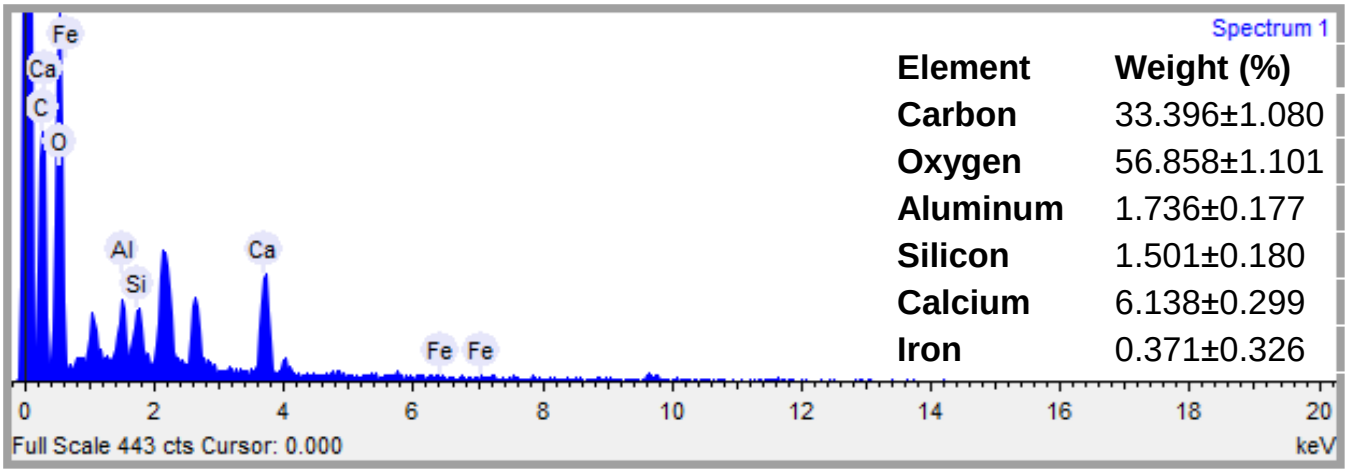

Fig. S6. EDX of F3 composed of 0.40% PF; 0.20% AS; 0.40% $CaCl_2$; 1% alginate. Concentrations expressed as percentages refer to weight by volume (w/v). Conditions: gold-sputtered dried beads; acceleration voltage = 15 kV; magnification = 6.00k×.

3.1.5 Complementary formulation selection process

Table S6. Qualitative and physical assessment of the formulations for bead production

Assessment Parameter	F1	F2	F3	F4	F5	F6	Notes
Component dispersion	High	High	High	High	Low	Low	Refers to mixing efficiency: High (no aggregates); Low (presence of aggregates)
Mixture homogeneity	Yes	Yes	Yes	Yes	No	No	Indicates if components remained fully dispersed after the mixing process
Visual precipitation	No	No	No	Yes	No	Yes	Presence of visible sediment or phase separation post-mixing
Dripping performance	Good	Excellent	Excellent	Good	Poor	Excellent	Based on 10 mL flow: Poor (>10 min); Good (~10 min); Excellent (<10 min)
Beads per 10 mL	190±5	189±1	201±5	204±4	223±8	251±7	Average yield per 10 mL of precursor solution
Morphological uniformity	Yes	Yes	Yes	Yes	No	Partial	Refers to the shape consistency and size distribution of the beads
Moisture content (%)	95.9	95.8	95.7	94.1	95.5	93.3	Calculated on a wet basis. Standard deviation (SD) < 0.01. N/A- Not Applicable
Dry mass per bead (mg)	0.87	1.02	1.12	1.66	0.98	0.85	Calculated as total dry mass divided by beads. SD < 0.01

Image of the formed wet spheres:

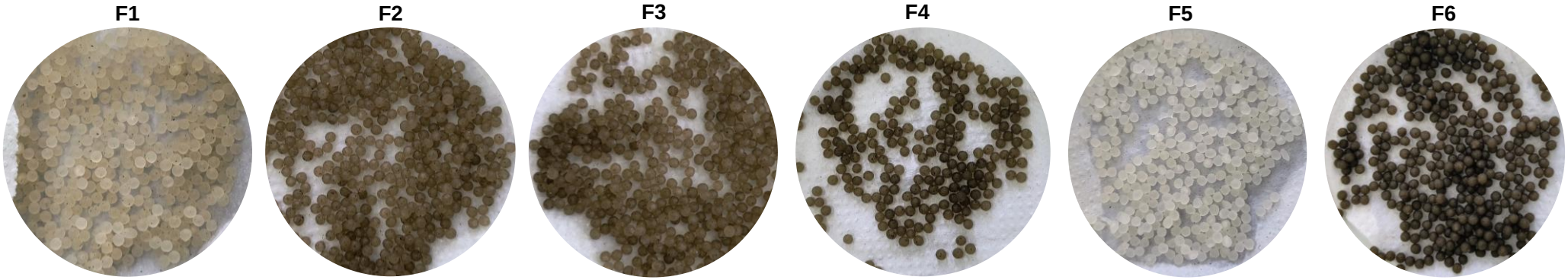

3.1.6 Thermal analysis (DSC-TGA)

Table S7. Thermal analysis (DSC-TGA) of the formed hybrid beads (F1 to F4)

Characteristic	**F1**	**F2**	**F3**	**F4**
Composition	0.03% PF 0.35% AS 0.80% $CaCl_2$ 1% alginate	0.40% PF 0.20% AS 0.70% $CaCl_2$ 1% alginate	0.40% PF 0.20% AS 0.40% $CaCl_2$ 1% alginate	1.50% PF 0.20% AS 0.40% $CaCl_2$ 1% alginate
Dehydration	12%	16%	20%	18%
Event at ~200 °C (DTG Peak)	Present and intense	Present and intense	Present and intense	Absent
Pyrolysis at ~370 °C (cellulose DTG peak)	Absent	Slight and evident. Endothermic (DSC)	Slight and evident. Endothermic (DSC)	Dominant and intense. Endothermic (DSC)
Char yield (%)	~40%	~30%	~30%	~23%
Onset temp (°C)	28.21	26.60	24.36	24.63
DTG peak (°C)	203.77	355.18	56.61	357.47
Tm,peak (°C)	200.00	67.92	65.59	65.05

Onset temp (°C): Temperature at which the mass falls below 99.5% of the initial value (adopted criterion). DTG Peak (°C): Temperature where the absolute value of the derivative weight is at its maximum, indicating the maximum rate of mass loss. Tm,peak (°C): Temperature of the primary peak in the DSC signal within the range. Concentrations expressed as percentages refer to weight by volume (w/v).

3.1.7 Apparent pore size distribution and Log-normal fitting

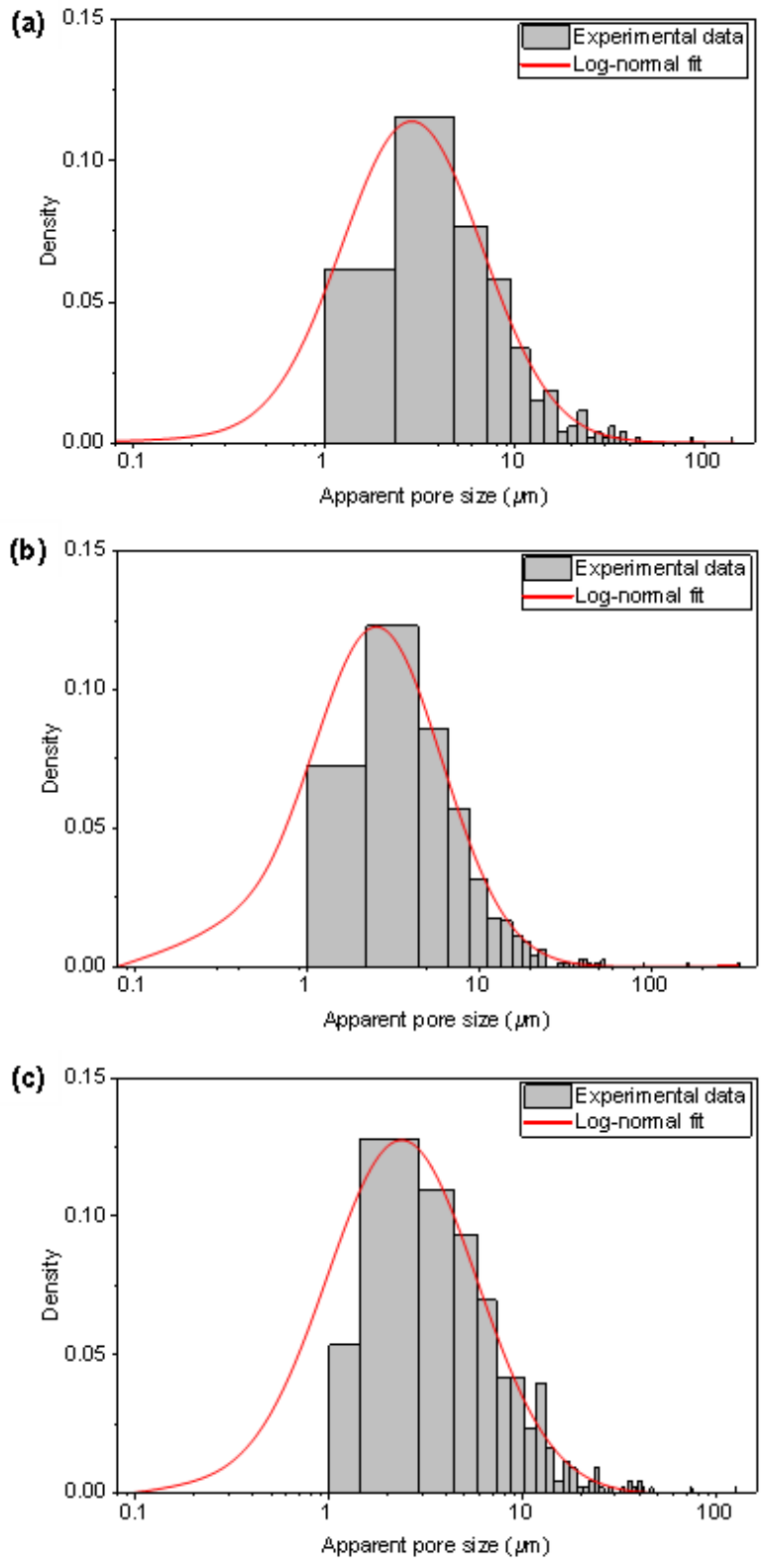

Fig. S7. Apparent pore size distribution and Log-normal fitting. Formulations: (a) F3, (b) F5, and (c) F6. The histograms represent the experimental data (density), and the red solid lines indicate the Log-normal probability density function fit. All distributions are plotted on a semi-logarithmic scale (x-axis) to highlight the microstructural heterogeneity and the presence of multiscale porosity. F3 (0.40% PF; 0.20% AS; 0.40% $CaCl_2$; 1% alginate); F5 (0.50% AS; 1.00% $CaCl_2$; 1% alginate); e F6 (1.50% PF; 1.00% $CaCl_2$; 1% alginate). Concentrations in (w/v).

3.1.8 Methylene blue adsorption assays

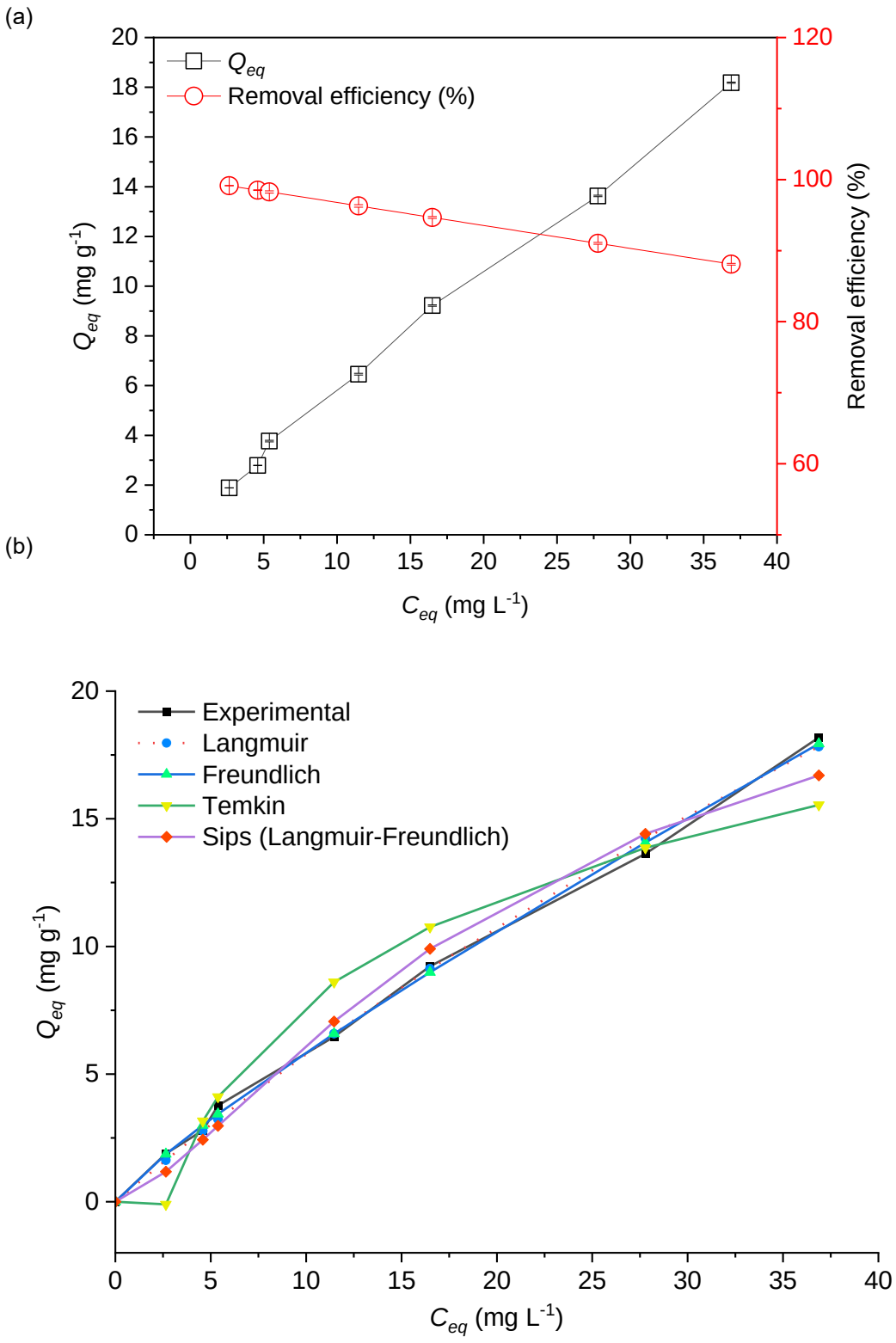

Fig. S8. Experimental results of the methylene blue (MB) adsorption isotherm: (a) Plot of adsorption capacity (Q) and removal efficiency versus initial MB concentration; (b) Fitting of experimental data to different adsorption isotherms. Q_{eq} is the equilibrium adsorption capacity, and C_{eq} is the equilibrium dye concentration. Conditions: initial (MB) = 31.00–310.00 mg L^{-1}; dosage = 18 wet beads (20 mg dry) per mL; pH = 6.98 ± 0.08; temperature = 292 K; time = 4 h.

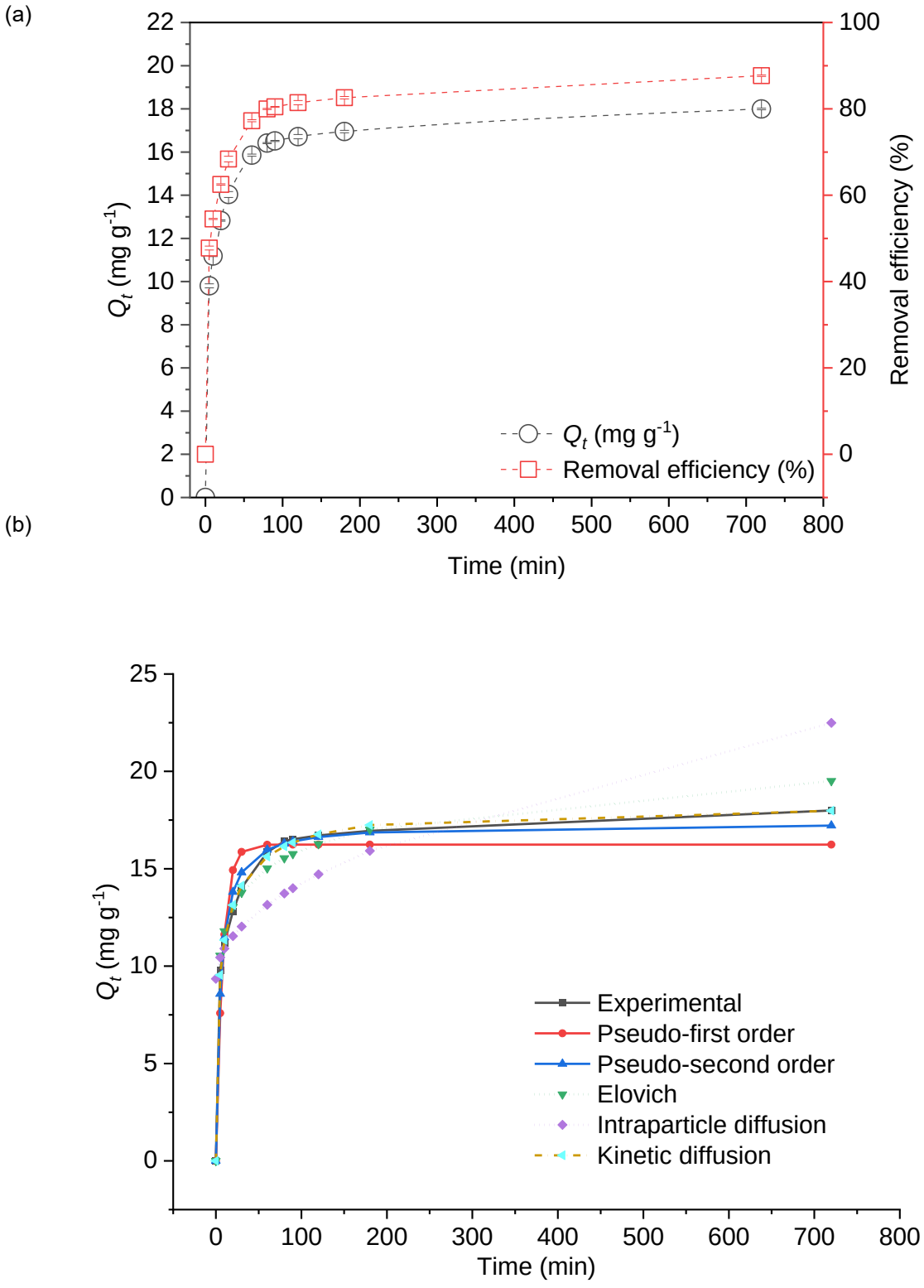

Fig. S9. Experimental results of methylene blue adsorption kinetics: (a) Plot of adsorption capacity (Q) and removal efficiency versus adsorption time; (b) Fitting of experimental data to different kinetic adsorption models. Q_t is the adsorption capacity as a function of time. Conditions: initial (MB) = 332.00 mg L^{-1}; dosage = 18 beads mL^{-1}; pH = 6.98 ± 0.08; temperature = 292 K; time = 5–720 min.

References supporting information

Holliday MC, Parsons DR, Zein SH (2024) Agricultural pea waste as a low-cost pollutant biosorbent for methylene blue removal: adsorption kinetics, isotherm and thermodynamic studies. Biomass Convers Biorefin 14:6671–6685. https://doi.org/10.1007/s13399-022-02865-8

Li G, Yu Y, Han W, Zhu L, Si T, Wang H, Li K, Sun Y, He Y (2021) Solvent evaporation self-motivated continual synthesis of versatile porous polymer microspheres via foaming-transfer. Colloids Surf A 615:126239. https://doi.org/10.1016/j.colsurfa.2021.126239

Mikolajczyk AP, Fortela DLB, Berry JC, Chirdon WM, Hernandez RA, Gang DD, Zappi ME (2024) Evaluating the suitability of linear and nonlinear regression approaches for the Langmuir adsorption model as applied toward biomass-based adsorbents: Testing residuals and assessing model validity. Langmuir 40:20428–20442. https://doi.org/10.1021/acs.langmuir.4c01786

Ostaszewski P, Długosz O, Banach M (2022) Analysis of measuring methods of the concentration of methylene blue in the sorption process in fixed-bed column. Int J Environ Sci Technol 19:1–8. https://doi.org/10.1007/s13762-021-03156-x

Vitek R, Masini JC (2023) Nonlinear regression for treating adsorption isotherm data to characterize new sorbents: Advantages over linearization demonstrated with simulated and experimental data. Heliyon 9:e15128. https://doi.org/10.1016/j.heliyon.2023.e15128

Wei Z, Liu L, Yang J, Dunn CB, Zhang T, Hong FF, Qiang Z, Ren J (2025) Ethanol-mediated freeze-drying enables robust bacterial cellulose aerogels for enhanced drug loading and hemostasis dressing. Carbohydr Polym 368:124091. https://doi.org/10.1016/j.carbpol.2025.124091